ASME Cold Plate Design Competition
Progress Report

May 20, 2025

Team Members:

Walid Sherif	202200702
Abdelrhman Alnaqeeb	202200281
Marwan Amr	202200050

Supervisors:

Dr. Ahmed Elatyar
Eng. Tarek Shaker

Institution:

Zewail City for Science and Technology

Contents

1 Problem Definition

1.1 Project Objective

The objective of this project is to design, analyze, and optimize an additively manufactured cold plate for cooling constant heat flux power electronics modules subjected to forced convection liquid cooling using water. The cold plate must efficiently dissipate 350 W of heat while minimizing thermal resistance, pressure drop, and material usage.

1.2 Design Requirements

Based on the competition guidelines, the cold plate design must meet the following requirements:

- Base plate size: $100 \times 80 \times 1.6$ mm
- Fin plate maximum volume: $75.5 \times 56.5 \times 3$ mm
- Minimum feature size: 0.1 mm
- Maximum feature size (XY): 0.5 mm
- Maximum feature size (Z): 3 mm, limited by cold plate fin volume
- Minimum feature resolution (XY): $33\frac{1}{3}\,\mu$m
- Minimum feature resolution (Z): $30\,\mu$m
- Minimum feature overhang angle: 20° (from XY plane)
- Material: Pure copper (thermal conductivity ~ 380 W/m·K)
- Flow configuration: Side-in Side-out
- Inlet/Outlet: 3/8" ID tube
- Flow rate: 1-2 L/min (0.5-1.0 GPM)
- Power load: 350 W
- Coolant inlet temperature: 20°C

1.3 Performance Metrics

The performance of the cold plate designs is evaluated using a Figure of Merit (FOM) defined as:

$$\text{FOM} = 0.4 \cdot \frac{R_{\text{th,ref}} - R_{\text{th}}}{R_{\text{th,ref}}} + 0.3 \cdot \frac{\Delta P_{\text{ref}} - \Delta P}{\Delta P_{\text{ref}}} + 0.3 \cdot \frac{m_{\text{solid}} - m}{m_{\text{solid}}}$$

Where:

- $R_{\text{th,ref}} = 0.1$ K/W (reference thermal resistance)
- $\Delta P_{\text{ref}} = 30$ kPa (reference pressure drop)
- $m_{\text{solid,ref}} = 114.7$ g (reference mass)

This FOM balances three key performance aspects:

1. Thermal performance (40% weight)
2. Hydraulic performance (30% weight)
3. Material efficiency (30% weight)

2 Physical Model and Geometry

2.1 Cold Plate Assembly

The cold plate assembly consists of the following components:
- Base plate ($100 \times 80 \times 1.6$ mm)
- Fin plate (maximum volume: $75.5 \times 56.5 \times 3$ mm)
- Housing with inlet and outlet ports
- Barb fittings for 3/8" ID tube connections

The assembly features a side-in side-out flow configuration with 3.5 mm accumulator sections at the ends of the fin plate to ensure uniform flow distribution.

2.2 Fin Design Concepts

Progress Report Comment: We were asked to design 10 concepts for the fins, and we would receive help to choose the most efficient one before carrying out the final simulation.

Ten different fin concepts were designed and evaluated:

1. Parallel Straight Fins

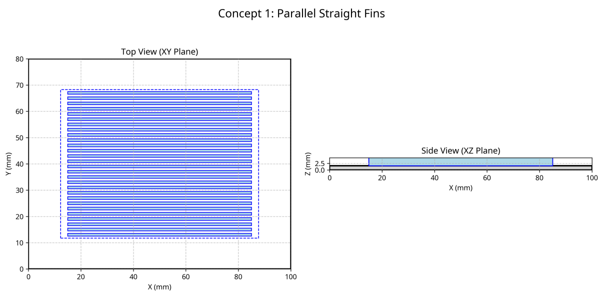

Figure 1: Parallel Straight Fins

2. Offset Strip Fins

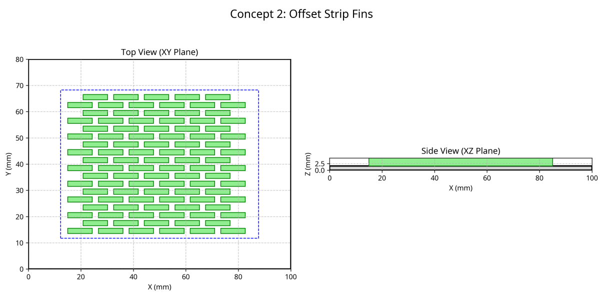

Figure 2: Offset Strip Fins

3. Pin Fin Array

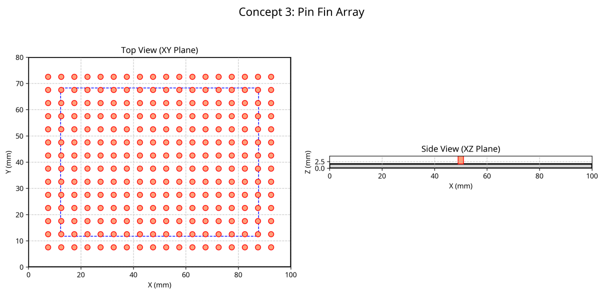

Figure 3: Pin Fin Array

4. Wavy Fins

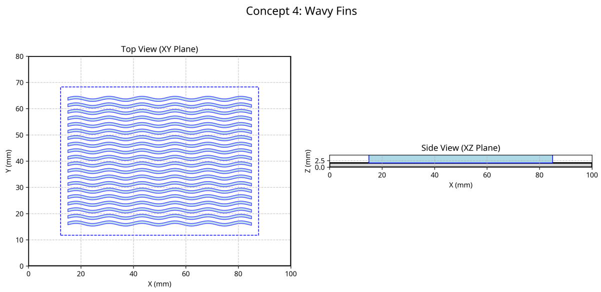

Figure 4: Wavy Fins

5. Herringbone Pattern

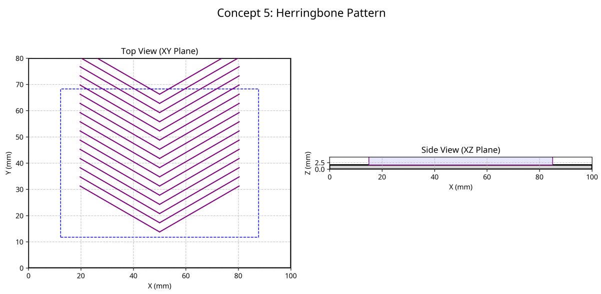

Figure 5: Herringbone Pattern

6. Micro-channel Fins

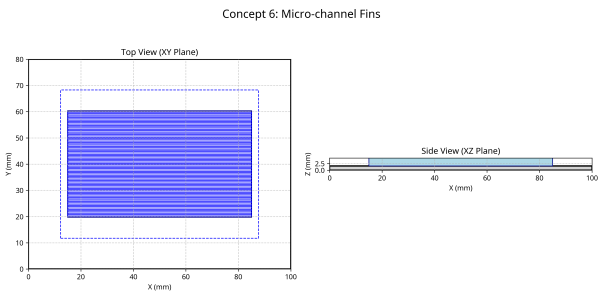

Figure 6: Micro-channel Fins

7. Honeycomb Structure

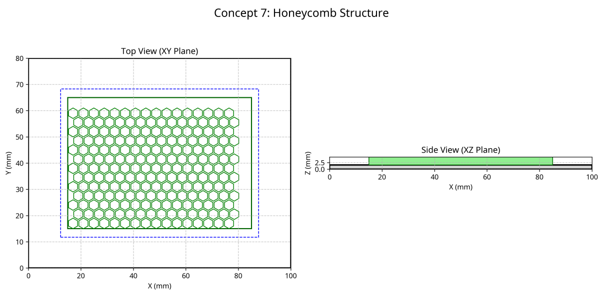

Figure 7: Honeycomb Structure

8. Radial Fins

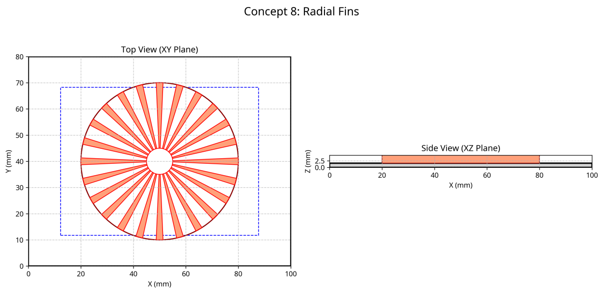

Figure 8: Radial Fins

9. Tapered Fins

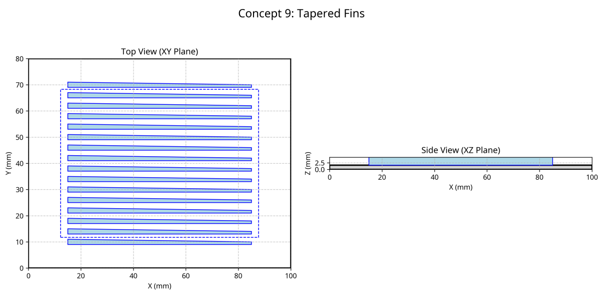

Figure 9: Caption

10. Hybrid Pin-Fin and Channel

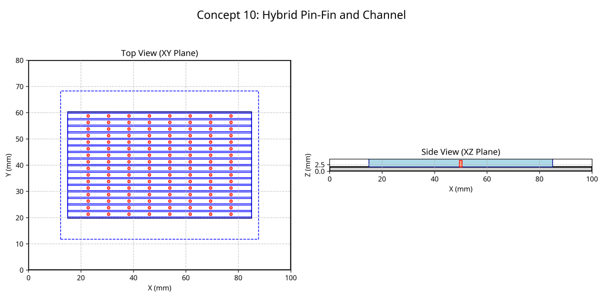

Figure 10: Hybrid Pin-Fin and Channel

3 Mathematical Model

3.1 Heat Transfer Modes

The cold plate design involves three primary heat transfer modes:

1. Conduction: Heat transfer through the solid copper material from the base plate to the fins.
2. Convection: Heat transfer from the fins to the water flowing through the channels.
3. Advection: Heat transfer due to the bulk motion of the water.

3.2 Thermal Resistance Network

The thermal resistance network for the cold plate consists of:

1. Conductive resistance through the base plate:

$$R_{\text{base}} = \frac{t_{\text{base}}}{k_{\text{copper}} \cdot A_{\text{base}}}$$

2. Conductive resistance through the fins:

$$R_{\text{fin}} = \frac{1}{\eta_{\text{fin}} \cdot h \cdot A_{\text{fin}}}$$

3. Convective resistance at the fluid-solid interface:

$$R_{\text{conv}} = \frac{1}{h \cdot A_{\text{total}}}$$

The total thermal resistance is the sum of these resistances in series:

$$R_{\text{total}} = R_{\text{base}} + R_{\text{fin}} + R_{\text{conv}}$$

3.3 Fluid Flow Model

The fluid flow through the cold plate is modeled using the following equations:

1. Continuity equation:
$$\nabla \cdot (\rho V) = 0$$

2. Momentum equation (Navier-Stokes):

$$\rho(V \cdot \nabla)V = -\nabla p + \mu \nabla^2 V$$

3. Energy equation:
$$\rho c_p (V \cdot \nabla)T = k \nabla^2 T$$

3.4 Pressure Drop Calculation

The pressure drop through the cold plate is calculated using the Darcy-Weisbach equation:

$$\Delta p = f \cdot \frac{L}{D_h} \cdot \frac{\rho V^2}{2}$$

For laminar flow ($Re < 2300$), the friction factor is calculated as:

$$f = \frac{64}{Re}$$

For turbulent flow ($Re > 2300$), the Blasius correlation is used:

$$f = 0.316 \cdot Re^{-0.25}$$

4 Simulation Methodology

4.1 Simulation Approach

The thermal and hydraulic performance of each fin concept was simulated using a combination of analytical models and numerical simulations. The simulation approach involved:

1. Creating geometric models of each fin concept
2. Defining material properties and boundary conditions
3. Calculating thermal resistance using fin theory and convective heat transfer correlations
4. Calculating pressure drop using fluid flow equations
5. Calculating mass based on the geometry and material density
6. Computing the Figure of Merit for each design

4.2 Boundary Conditions

The following boundary conditions were applied in the simulations:
- Thermal boundary conditions:
- Uniform heat flux of 350 W at the bottom surface of the base plate
- Inlet water temperature of 20°C
- Adiabatic (insulated) outer walls
- Hydraulic boundary conditions:
- Flow rate of 0.75 GPM (average of the specified range)
- Atmospheric pressure at the outlet
- No-slip condition at the walls

5 Results and Discussion

5.1 Simulation Results

The simulation results for all 10 fin concepts are summarized in the table below:

Rank	Concept	Design	FOM	Thermal Resistance (K/W)	Pressure Drop (kPa)	Mass (g)	Max Temp (°C)
1	C10	Hybrid Pin-Fin and Channel	0.5317	0.0214	3.50	132.93	27.49
2	C6	Micro-channel Fins	0.5241	0.0037	6.01	153.26	21.31
3	C8	Radial Fins	0.4836	0.0379	0.03	139.32	33.27
4	C4	Wavy Fins	0.4801	0.0243	0.44	159.85	28.52
5	C3	Pin Fin Array	0.4698	0.0436	0.00	135.97	35.27
6	C1	Parallel Straight Fins	0.4684	0.0221	0.56	167.37	27.72
7	C9	Tapered Fins	0.4390	0.0353	0.16	159.85	32.36
8	C2	Offset Strip Fins	0.4367	0.0265	1.57	168.88	29.27
9	C5	Herringbone Pattern	0.4237	0.0342	0.33	166.83	31.96
10	C7	Honeycomb Structure	0.3808	0.0563	0.01	150.66	39.70

Table 1: Summary of Simulation Results for All Fin Concepts

Progress Report Comment: These are not final simulations, they are merely simple simulations (done in python) for each fin concept and a ranking based on these simulations to choose the most optimal concept design. Once confirmed that we can go ahead with the chosen fin concept, a simulation would be done over the final assembly (which is the only part remaining in the project).

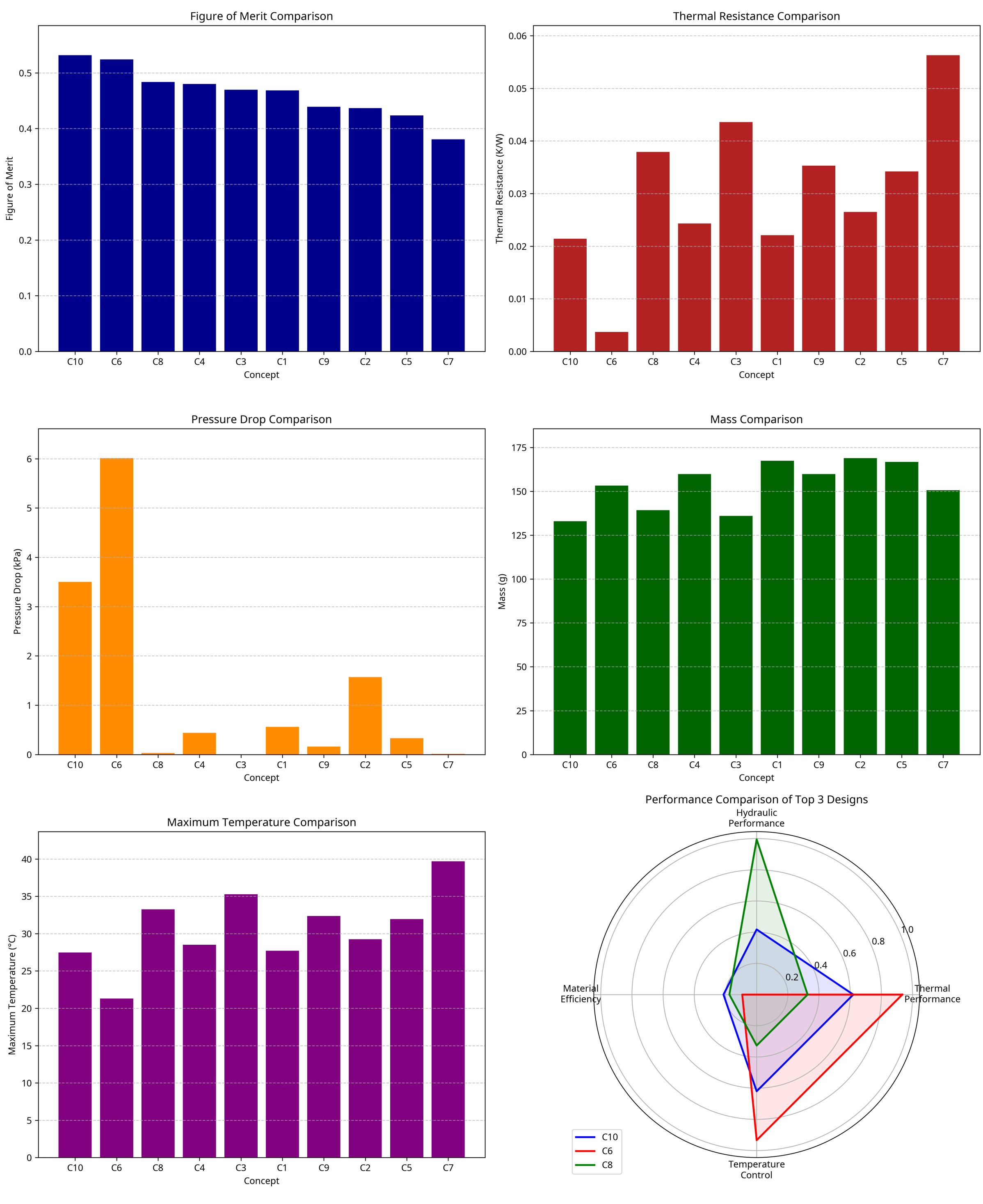

Figure 11: performance comparison

5.2 Performance Analysis

5.2.1 Thermal Performance

The Micro-channel Fins design (C6) achieved the lowest thermal resistance (0.0037 K/W) and consequently the lowest maximum temperature (21.31°C). The Hybrid Pin-Fin and Channel design (C10) achieved the second-best thermal performance with a thermal resistance of 0.0214 K/W and a maximum temperature of 27.49°C.

5.2.2 Hydraulic Performance

The Pin Fin Array (C3) and Honeycomb Structure (C7) designs had the lowest pressure drops (approximately 0 kPa), indicating minimal flow resistance. The Micro-channel Fins design (C6) had the highest pressure drop (6.01 kPa) due to the narrow channels.

5.2.3 Material Efficiency

The Hybrid Pin-Fin and Channel design (C10) had one of the lowest masses (132.93 g), which is only 16% higher than the reference mass of 114.7 g.

5.3 Fin selected

Based on the ranking in table 1, we select concept 10 - Hybrid Fin-Pins.

6 Part 1: Analysis & Simulation of selected fin design

Parameters

- ρ_0: Design variable ($0 \leq \rho_0 \leq 1$)
- C_p: Specific heat capacity
- $\mathbf{u}$: Velocity vector
- T: Temperature
- k_s, k_f: Thermal conductivities (solid, fluid)
- H: Heat generation coefficient
- T_r: Reference temperature
- T_0: Boundary temperature at $x = 0$
- L: Domain length

Our geometry looks as follows:

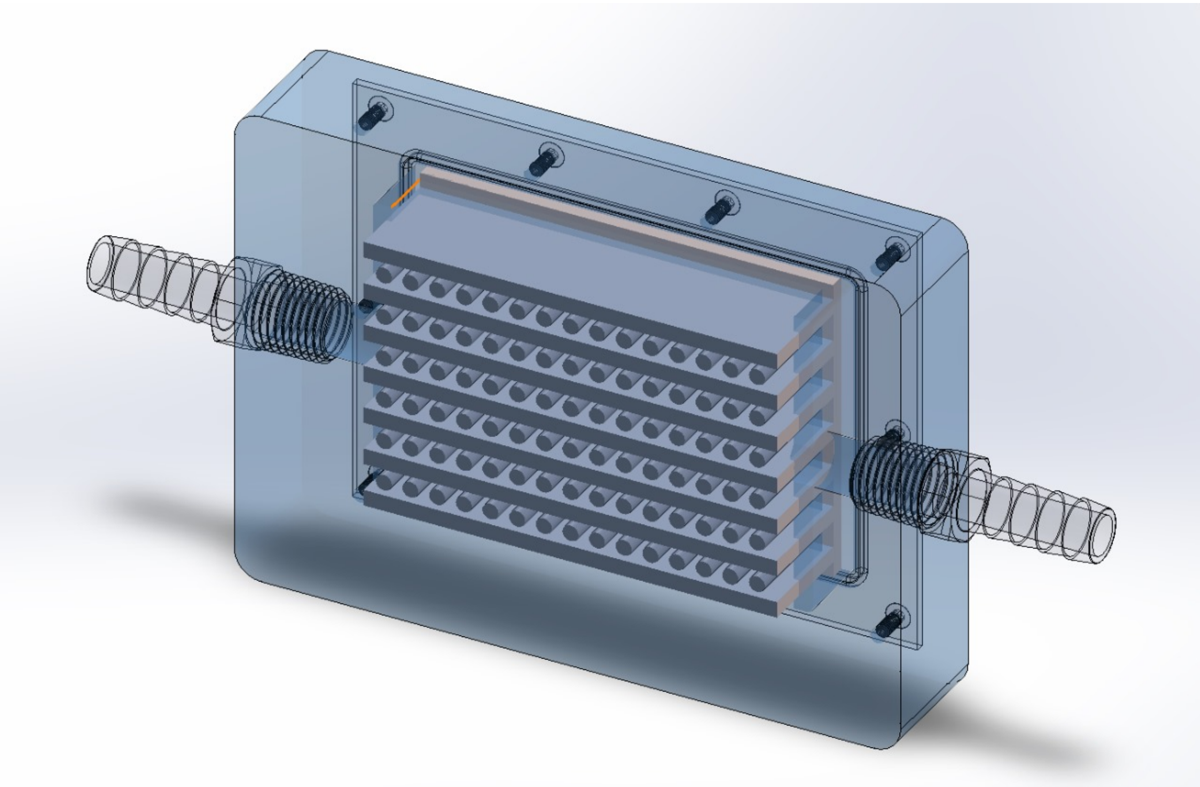

Figure 12: Hybrid Fin-Pins (displayed on SOLIDWORKS 2021)

We import it into COMSOL Multiphysics and define our boundary conditions. But first, we need to modify the geometry by introducing a block inside the cold plate and setting it's material to water (with a velocity of $1cm/s$. (figure 13)

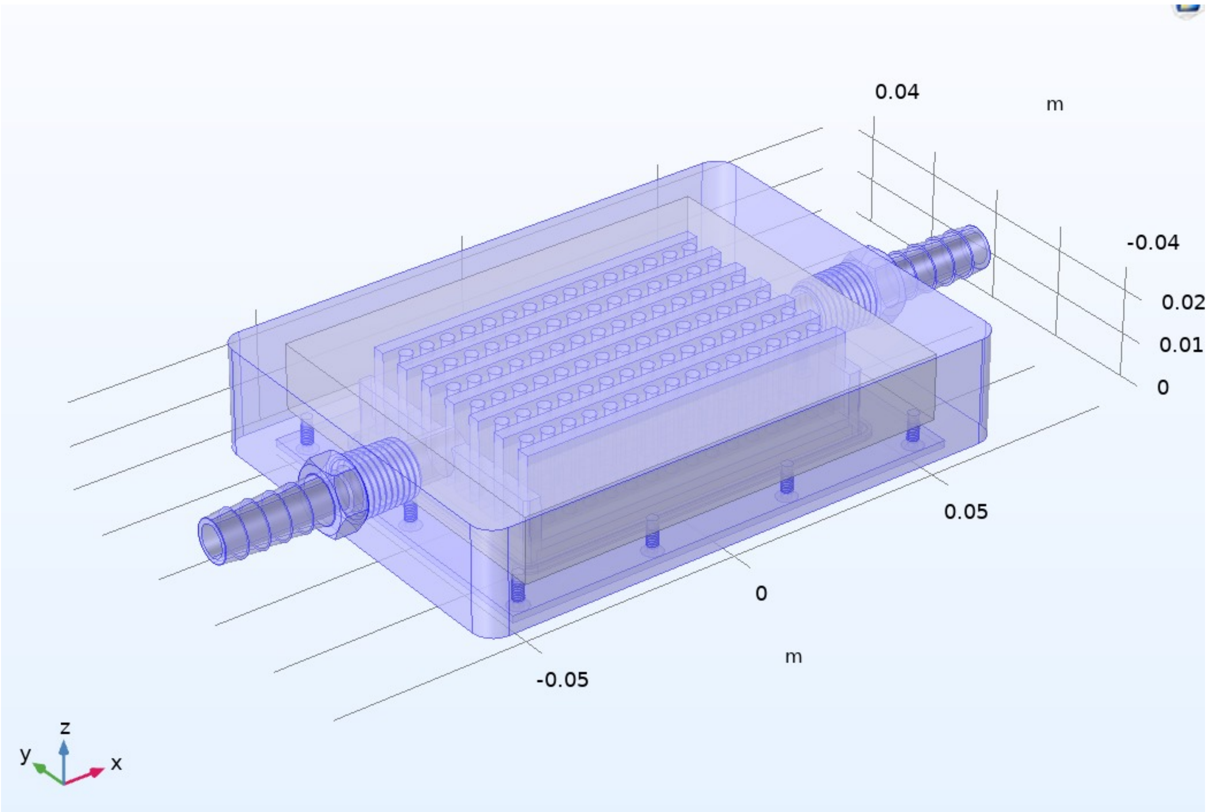

Figure 13: Boundary conditions: convective heat flux on plate walls and fins, temperature of 350K at base. Cold plate material is copper (as instructed by competition guidelines).

6.1 Mesh

We use a physics-controlled mesh generated on COMSOL Multiphysics 6.0 shown below:

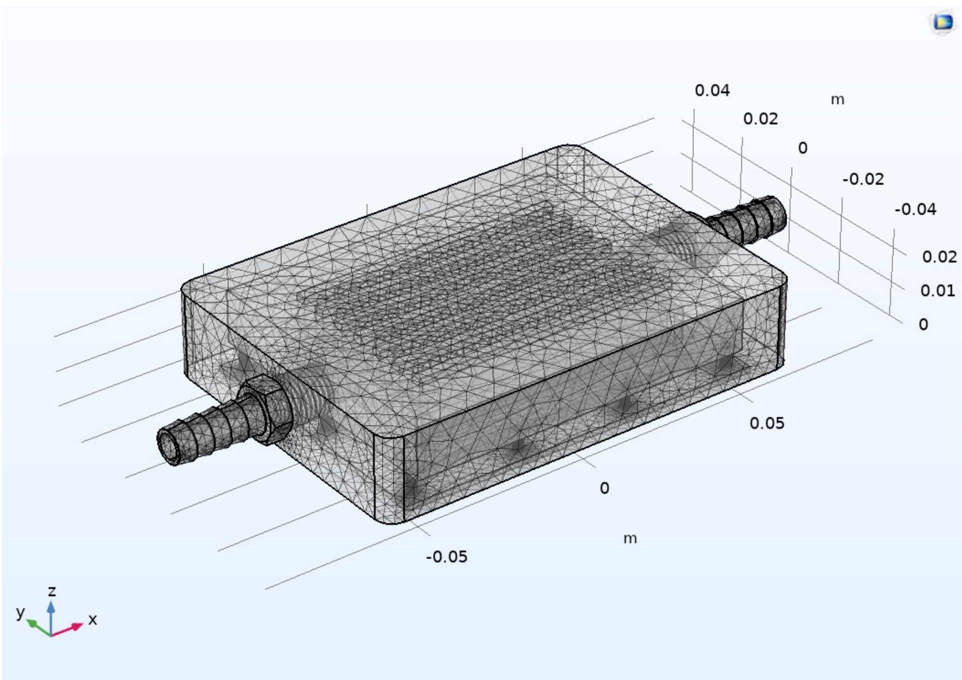

Figure 14: Meshing

Simulation results will be compared to theoretical results at section 8.

First, we need to get some analytical results to compare simulation results to. The reason we do that is we dont have experimental data to compare with.

We're interested in many things. Let's start with tempurature variation with distance $T(x) vs x$. Consider the 1-D energy equation:

$$(1-\rho)\rho C_p(\mathbf{u}\cdot\nabla T) = \nabla\cdot\left[\left(\rho k_s + (1-\rho)k_f\right)\nabla T\right] + \rho H(T_r - T) \tag{1}$$

Neglecting Convection

$$\nabla\cdot\left[\left(\rho k_s + (1-\rho)k_f\right)\nabla T\right] + \rho H(T_r - T) = 0 \tag{2}$$

Constant $\rho = \rho_0$

$$\frac{d}{dx}\left[k(\rho_0)\frac{dT}{dx}\right] + \rho_0 H(T_r - T) = 0 \tag{3}$$

Where:

$$k(\rho_0) = \rho_0 k_s + (1-\rho_0)k_f \tag{4}$$

Simplify:

$$k(\rho_0)\frac{d^2T}{dx^2} + \rho_0 H(T_r - T) = 0 \tag{5}$$

Rearrange:

$$\frac{d^2T}{dx^2} - \frac{\rho_0 H}{k(\rho_0)}T = -\frac{\rho_0 H}{k(\rho_0)}T_r \tag{6}$$

Define:

$$\alpha^2 = \frac{\rho_0 H}{k(\rho_0)} \tag{7}$$

Thus:

$$\frac{d^2T}{dx^2} - \alpha^2 T = -\alpha^2 T_r \tag{8}$$

General Solution

Homogeneous solution:

$$T_h(x) = Ae^{\alpha x} + Be^{-\alpha x} \tag{9}$$

Particular solution:

$$T_p = T_r \tag{10}$$

General solution:

$$T(x) = Ae^{\alpha x} + Be^{-\alpha x} + T_r \tag{11}$$

Boundary Conditions

- At $x = 0$: $T(0) = T_0$
- At $x = L$: $\frac{dT}{dx}(L) = 0$

Apply:

$$T(0) = A + B + T_r = T_0 \tag{12}$$

$$A + B = T_0 - T_r \tag{13}$$

Derivative:

$$\frac{dT}{dx} = \alpha A e^{\alpha x} - \alpha B e^{-\alpha x} \tag{14}$$

At $x = L$:

$$\frac{dT}{dx}(L) = \alpha A e^{\alpha L} - \alpha B e^{-\alpha L} = 0 \tag{15}$$

$$A e^{\alpha L} = B e^{-\alpha L} \tag{16}$$

$$A = B e^{-2\alpha L} \tag{17}$$

Solving for Constants

Substitute:

$$B e^{-2\alpha L} + B = T_0 - T_r \tag{18}$$

$$B(e^{-2\alpha L} + 1) = T_0 - T_r \tag{19}$$

$$B = \frac{T_0 - T_r}{1 + e^{-2\alpha L}} \tag{20}$$

$$A = \frac{(T_0 - T_r)e^{-2\alpha L}}{1 + e^{-2\alpha L}} = \frac{T_0 - T_r}{1 + e^{2\alpha L}} \tag{21}$$

Final Temperature Profile

$$T(x) = \frac{T_0 - T_r}{1 + e^{2\alpha L}} e^{\alpha x} + \frac{T_0 - T_r}{1 + e^{-2\alpha L}} e^{-\alpha x} + T_r \tag{22}$$

Where:

$$\alpha = \sqrt{\frac{\rho_0 H}{k(\rho_0)}} \tag{23}$$

$$k(\rho_0) = \rho_0 k_s + (1 - \rho_0) k_f \tag{24}$$

2nd, we are also interested in the maximum temperature vs. inlet pressure. **We are only interested in this for the 2nd part of the project**, as the first part's coplate wasn't by our design and would yield huge error. These errors are demonstrated in section 8.

Governing Equations

Please note the subscript 'b' is for the heat source, as the heat source is taken as a battery.
Energy Equation (Coolant, Steady-State):

$$\rho_c C_{pc}(\mathbf{u}_c \cdot \nabla T_c) = k_c \nabla^2 T_c \tag{25}$$

Heat Source (HS) Energy Equation (Steady-State):

$$\nabla \cdot (k_b \nabla T_b) + Q_b = 0 \tag{26}$$

Where $Q_b = 240\,\mathrm{kW/m^3}$.

Flow Equations:

$$\nabla \cdot (\rho_c \mathbf{u}_c) = 0 \tag{27}$$

$$\rho_c(\mathbf{u}_c \cdot \nabla)\mathbf{u}_c = -\nabla p_c + \mu_c \nabla^2 \mathbf{u}_c \tag{28}$$

Simplified HS Energy Equation (1D)

$$k_b \frac{d^2 T_b}{dz^2} + Q_b = 0 \tag{29}$$

Solution:

$$T_b(z) = -\frac{Q_b}{2k_b} z^2 + C_1 z + C_2 \tag{30}$$

Boundary conditions:

- At $z = 0$: $-k_b \frac{dT_b}{dz} = h_c(T_b - T_c)$
- At $z = L_b$: $\frac{dT_b}{dz} \approx 0$

Constants:

$$C_1 \approx \frac{Q_b L_b}{k_b}, \quad C_2 = T_c - \frac{Q_b L_b}{h_c} \tag{31}$$

Maximum temperature:

$$T_{b,\max} = T_c + \frac{Q_b L_b^2}{2k_b} - \frac{Q_b L_b}{h_c} \tag{32}$$

Heat Transfer Coefficient

$$h_c = \frac{\rho_c C_{pc} u_{\text{in}} A_{\text{in}} (T_{\text{out}} - T_{\text{in}})}{A_c \left(T_{\text{cw,ave}} - \frac{T_{\text{out}} + T_{\text{in}}}{2}\right)} \tag{33}$$

$$Nu = \frac{h_c D_h}{k_c} \tag{34}$$

Velocity relation:

$$u_{\text{in}} \propto \sqrt{p_{\text{in}}} \tag{35}$$

Heat transfer coefficient:

$$h_c = h_0 \sqrt{\frac{p_{\text{in}}}{p_0}} \tag{36}$$

Where $p_0 = 150\,\mathrm{Pa}$, h_0: Calibration:

$$\frac{Q_b L_b}{h_0} = T_c + \frac{Q_b L_b^2}{2k_b} - T_{b,\max} \tag{37}$$

Final Expression

$$T_{b,\max}(p_{\text{in}}) = 298 + 1107.7 - \frac{1440}{h_0}\sqrt{\frac{150}{p_{\text{in}}}} \tag{38}$$

Parameters:

- $T_c = 298\,\text{K}$, $Q_b = 240 \times 10^3\,\text{W/m}^3$
- $L_b = 0.006\,\text{m}$, $k_b = 3.9\,\text{W/m·K}$

7 Part 2: Topology optimized channel design

Consider a cold plate with inlet and outlet that looks like this:

Figure 15: Cold plate (without channels)

We want to create a topology for the channels that maximizes heat transfer for the cold plate, to do that, we can use concepts from linear & non-linear programming and solve the maximization problem, which then gives us the topology needed.

7.1 Optimization Problem (Optional read)

This part requires knowledge in Calculus of Variations & Optimization theory, therefore this section can be skipped, it's only here for proof of work. Consider the following optimization problem:

$$J = \int_\Omega \rho\, H(T_r - T)\, d\Omega \tag{39}$$

which is equivalent to minimizing:

$$J = -\int_\Omega \rho\, H(T_r - T)\, d\Omega \tag{40}$$

where $\rho = \rho(x) \in [0, 1]$ is the design variable.

Subject to the following partial differential constraints:

1. **Incompressible flow:**
$$\nabla \cdot \mathbf{u} = 0 \tag{41}$$
2. **Steady-state Navier-Stokes momentum equation:**
$$\rho(\mathbf{u} \cdot \nabla)\mathbf{u} = -\nabla p + \mu \nabla^2 \mathbf{u} - \alpha(\rho)\mathbf{u} \tag{42}$$

3. **Steady-state energy equation with conduction and convection:**

$$(1-\rho)\rho C_p(\mathbf{u}\cdot\nabla T) = \nabla\cdot(k(\rho)\nabla T) + \rho H(T_r - T) \tag{43}$$

4. **Volume constraint:**

$$\int_\Omega \rho\, d\Omega \le V_s \tag{44}$$

To maximize the functional $J = \int_\Omega \rho H(T_r - T)\, d\Omega$, we use the adjoint method to derive the first-order optimality conditions (Karush-Kuhn-Tucker or KKT conditions).

Since this is a PDE-constrained optimization problem, we formulate the Lagrangian by introducing adjoint variables for each constraint and a Lagrange multiplier for the volume constraint.

- **Objective functional**: $J = -\int_\Omega \rho H(T_r - T)\, d\Omega$.
- **Adjoint variables**:
  - For $\nabla\cdot u = 0$, introduce $q(x)$, a scalar field (adjoint pressure).
  - For the momentum equation $\rho(u\cdot\nabla)u = -\nabla p + \mu\nabla^2 u - \alpha(\rho)u$, introduce $v(x)$, a vector field (adjoint velocity).
  - For the energy equation $(1-\rho)\rho C_p(u\cdot\nabla T) = \nabla\cdot(k(\rho)\nabla T) + \rho H(T_r - T)$, introduce $\theta(x)$, a scalar field (adjoint temperature).
- **Lagrange multiplier**: For the volume constraint $\int_\Omega \rho\, d\Omega \le V_s$, introduce λ, a scalar with $\lambda \ge 0$, and the complementary slackness condition $\lambda\left(\int_\Omega \rho\, d\Omega - V_s\right) = 0$.

The Lagrangian $\mathcal{L}$ is:

$$\mathcal{L} = -\int_\Omega \rho H(T_r - T)\, d\Omega + \int_\Omega q(\nabla\cdot u)\, d\Omega + \int_\Omega v\cdot\left[\rho(u\cdot\nabla)u + \nabla p - \mu\nabla^2 u + \alpha(\rho)u\right]\, d\Omega + \int_\Omega \theta\left[(1-\rho)\rho C_p(u\right.$$

Step 3: Derive the First-Order Optimality Conditions

To find the optimality conditions we take the variations of $\mathcal{L}$ with respect to all variables $(\rho, u, T, p, v, q, \theta)$ and set each to zero.

p appears only in the momentum term: $\int_\Omega v\cdot\nabla p\, d\Omega$.

$$\delta_p\mathcal{L} = \int_\Omega v\cdot\nabla(\delta p)\, d\Omega$$

Integrate by parts:

$$\int_\Omega v\cdot\nabla(\delta p)\, d\Omega = -\int_\Omega (\nabla\cdot v)\delta p\, d\Omega + \int_{\partial\Omega} (v\cdot n)\delta p\, dS$$

Assuming boundary terms vanish (e.g., $v = 0$ on $\partial\Omega$), we get:

$$\delta_p \mathcal{L} = -\int_\Omega (\nabla \cdot v)\delta p \, d\Omega = 0$$

For arbitrary δp:

$$\nabla \cdot v = 0$$

This is the adjoint incompressibility condition.

T appears in the objective and energy terms:

- Objective: $-\int_\Omega \rho H(T_r - T)\, d\Omega$
- Energy: $\int_\Omega \theta \left[(1-\rho)\rho C_p (u \cdot \nabla T) - \nabla \cdot (k(\rho)\nabla T) - \rho H(T_r - T)\right] d\Omega$

$$\delta_T \mathcal{L} = -\int_\Omega \rho \delta H(T_r - T)\, d\Omega + \int_\Omega \theta \left[(1-\rho)\rho C_p (u \cdot \nabla(\delta T)) - \nabla \cdot (k(\rho)\nabla(\delta T)) - \rho \delta H(T_r - T)\right] d\Omega$$

Since $\delta H(T_r - T) = H'(T_r - T)(0 - \delta T) = -\delta(T_r - T)\delta T$:

- Objective term: $-\int_\Omega \rho(-\delta(T_r - T)\delta T)\, d\Omega = \int_\Omega \rho\delta(T_r - T)\delta T\, d\Omega$
- Energy source term: $-\int_\Omega \theta\rho(-\delta(T_r - T)\delta T)\, d\Omega = \int_\Omega \theta\rho\delta(T_r - T)\delta T\, d\Omega$

Now handle the derivative terms:

1. Convection: $\int_\Omega \theta(1-\rho)\rho C_p (u \cdot \nabla(\delta T))\, d\Omega$
   - Since $\nabla \cdot u = 0$, $u \cdot \nabla(\delta T) = \nabla \cdot (u\delta T)$.
   - $\int_\Omega \theta(1-\rho)\rho C_p \nabla \cdot (u\delta T)\, d\Omega = -\int_\Omega \nabla \cdot [\theta(1-\rho)\rho C_p u]\delta T\, d\Omega +$ boundary terms
   - Boundary terms vanish (e.g., $u \cdot n = 0$ or $\delta T = 0$ on $\partial\Omega$).
2. Diffusion: $\int_\Omega \theta[-\nabla \cdot (k(\rho)\nabla(\delta T))]\, d\Omega$
   - $\int_\Omega \theta\nabla \cdot (k(\rho)\nabla(\delta T))\, d\Omega = \int_\Omega \nabla\theta \cdot (k(\rho)\nabla(\delta T))\, d\Omega - \int_{\partial\Omega} \theta k(\rho)\frac{\partial \delta T}{\partial n}\, dS$
   - Boundary term vanishes.
   - $\int_\Omega \nabla\theta \cdot (k(\rho)\nabla(\delta T))\, d\Omega = -\int_\Omega \delta T \nabla \cdot (k(\rho)\nabla\theta)\, d\Omega$

So:

$$\delta_T \mathcal{L} = \int_\Omega \left[\rho\delta(T_r - T) + \theta\rho\delta(T_r - T) - \nabla \cdot [\theta(1-\rho)\rho C_p u] + \nabla \cdot (k(\rho)\nabla\theta)\right] \delta T\, d\Omega$$

Set to zero:

$$\nabla \cdot (k(\rho)\nabla\theta) - \nabla \cdot [\theta(1-\rho)\rho C_p u] + \rho(1+\theta)\delta(T_r - T) = 0$$

$$\nabla \cdot (k(\rho)\nabla\theta) - \nabla \cdot [\theta(1-\rho)\rho C_p u] = -\rho(1+\theta)\delta(T_r - T)$$

This is the adjoint energy equation.

u appears in all three constraints:

- Incompressibility: $\int_\Omega q(\nabla \cdot u)\, d\Omega$
- Momentum: $\int_\Omega v \cdot [\rho(u \cdot \nabla)u - \mu\nabla^2 u + \alpha(\rho)u]\, d\Omega$
- Energy: $\int_\Omega \theta(1-\rho)\rho C_p(u \cdot \nabla T)\, d\Omega$

$$\delta_u \mathcal{L} = \int_\Omega q(\nabla \cdot \delta u)\, d\Omega + \int_\Omega v \cdot [\rho(\delta u \cdot \nabla)u + \rho(u \cdot \nabla)\delta u - \mu\nabla^2 \delta u + \alpha(\rho)\delta u]\, d\Omega + \int_\Omega \theta(1-\rho)\rho C_p(\delta u \cdot \nabla T)\, d\Omega$$

1. Incompressibility: $\int_\Omega q\nabla \cdot \delta u\, d\Omega = -\int_\Omega (\nabla q) \cdot \delta u\, d\Omega$
2. Convective terms: $\int_\Omega v \cdot [\rho((\delta u \cdot \nabla)u + (u \cdot \nabla)\delta u)]\, d\Omega$
   - $\int_\Omega v \cdot [(u \cdot \nabla)\delta u]\, d\Omega = -\int_\Omega \delta u \cdot (u \cdot \nabla v)\, d\Omega$ (since $\nabla \cdot u = 0$)
   - $\int_\Omega v \cdot [(\delta u \cdot \nabla)u]\, d\Omega = \int_\Omega \delta u \cdot [(\nabla u)^T v]\, d\Omega$
   - Total: $\int_\Omega \delta u \cdot \rho[-(u \cdot \nabla)v + (\nabla u)^T v]\, d\Omega$
3. Viscous term: $\int_\Omega v \cdot [-\mu\nabla^2 \delta u]\, d\Omega = \int_\Omega \mu\nabla v : \nabla\delta u\, d\Omega = -\int_\Omega \mu(\nabla^2 v) \cdot \delta u\, d\Omega$
4. Damping: $\int_\Omega v \cdot [\alpha(\rho)\delta u]\, d\Omega = \int_\Omega \alpha(\rho) v \cdot \delta u\, d\Omega$
5. Energy: $\int_\Omega \theta(1-\rho)\rho C_p(\delta u \cdot \nabla T)\, d\Omega$

$$\delta_u \mathcal{L} = \int_\Omega \delta u \cdot \left[-\nabla q + \rho[-(u \cdot \nabla)v + (\nabla u)^T v] + \mu\nabla^2 v + \alpha(\rho)v + \theta(1-\rho)\rho C_p \nabla T\right]\, d\Omega$$

Set to zero:

$$-\nabla q + \rho[-(u \cdot \nabla)v + (\nabla u)^T v] + \mu\nabla^2 v + \alpha(\rho)v + \theta(1-\rho)\rho C_p \nabla T = 0$$

$$\rho[-(u \cdot \nabla)v + (\nabla u)^T v] + \mu\nabla^2 v + \alpha(\rho)v - \nabla q = -\theta(1-\rho)\rho C_p \nabla T$$

This is the adjoint momentum equation.

ρ appears in the objective, momentum, energy, and volume terms:

- Objective: $\delta_\rho J = -\int_\Omega \delta\rho H(T_r - T)\, d\Omega$
- Momentum: $\int_\Omega v \cdot [\delta\rho(u \cdot \nabla)u - \alpha'(\rho)\delta\rho u]\, d\Omega$
- Energy: $\int_\Omega \theta\left[(1-2\rho)\delta\rho C_p(u \cdot \nabla T) - \nabla \cdot (k'(\rho)\delta\rho\nabla T) - \delta\rho H(T_r - T)\right]\, d\Omega$
- Volume: $\lambda \int_\Omega \delta\rho\, d\Omega$

Energy diffusion term: $\int_\Omega \theta[-\nabla \cdot (k'(\rho)\delta\rho\nabla T)]\, d\Omega = \int_\Omega k'(\rho)\delta\rho(\nabla\theta \cdot \nabla T)\, d\Omega$.

$$\delta_\rho \mathcal{L} = \int_\Omega \delta\rho\left[-H(T_r - T) + v \cdot (u \cdot \nabla)u - \alpha'(\rho)v \cdot u + \theta C_p(1-2\rho)(u \cdot \nabla T) + k'(\rho)(\nabla\theta \cdot \nabla T) - \theta H(T_r -\right.$$

Set to zero:

$$v \cdot (u \cdot \nabla)u - \alpha'(\rho)v \cdot u + \theta C_p(1-2\rho)(u \cdot \nabla T) + k'(\rho)(\nabla\theta \cdot \nabla T) - (1+\theta)H(T_r - T) + \lambda = 0$$

This is the optimality condition, with $\lambda \geq 0$ satisfying the volume constraint.

Primal Equations

$$\nabla \cdot u = 0$$
$$\rho(u \cdot \nabla)u = -\nabla p + \mu\nabla^2 u - \alpha(\rho)u$$
$$(1-\rho)\rho C_p(u \cdot \nabla T) = \nabla \cdot (k(\rho)\nabla T) + \rho H(T_r - T)$$

Adjoint Equations

$$\nabla \cdot v = 0$$
$$\rho[-(u \cdot \nabla)v + (\nabla u)^T v] + \mu\nabla^2 v + \alpha(\rho)v - \nabla q = -\theta(1-\rho)\rho C_p \nabla T$$
$$\nabla \cdot (k(\rho)\nabla\theta) - \nabla \cdot [\theta(1-\rho)\rho C_p u] = -\rho(1+\theta)\delta(T_r - T)$$

Optimality Condition

$v \cdot (u \cdot \nabla)u - \alpha'(\rho)v \cdot u + \theta C_p(1-2\rho)(u \cdot \nabla T) + k'(\rho)(\nabla\theta \cdot \nabla T) - (1+\theta)H(T_r - T) + \lambda = 0$
With $\lambda \geq 0$, $\int_\Omega \rho \, d\Omega \leq V_s$, and $\lambda \left(\int_\Omega \rho \, d\Omega - V_s\right) = 0$.

Update Rule for $\rho(x)$

Define the sensitivity:

$s(\rho) = v \cdot (u \cdot \nabla)u - \alpha'(\rho)v \cdot u + \theta C_p(1-2\rho)(u \cdot \nabla T) + k'(\rho)(\nabla\theta \cdot \nabla T) - (1+\theta)H(T_r - T)$

Then:

$$s(\rho) + \lambda = 0$$

In topology optimization, $\rho(x)$ is updated iteratively. Since $\rho \in [0,1]$, a common approach (e.g., optimality criteria method) adjusts ρ based on $s(\rho)$, with λ determined to satisfy the volume constraint. Symbolically, the update direction is opposite to the sensitivity (to minimize J), but constrained:

- If $s(\rho) < 0$, increase ρ (since $\frac{\partial \mathcal{L}}{\partial \rho} < 0$).
- If $s(\rho) > 0$, decrease ρ.
- Adjust λ to enforce $\int_\Omega \rho \, d\Omega = V_s$ (if equality is assumed).

Numerically, this requires an iterative solver (e.g., gradient descent with projection), but symbolically:

$$\rho_{\text{new}}(x) = \max\left(0, \min\left(1, \rho_{\text{old}}(x) - \eta(s(\rho) + \lambda)\right)\right)$$

where $\eta > 0$ is a step size, and λ is tuned at each iteration. Which we do in COMSOL, and the results from optimizing the structure in figure 15 is:

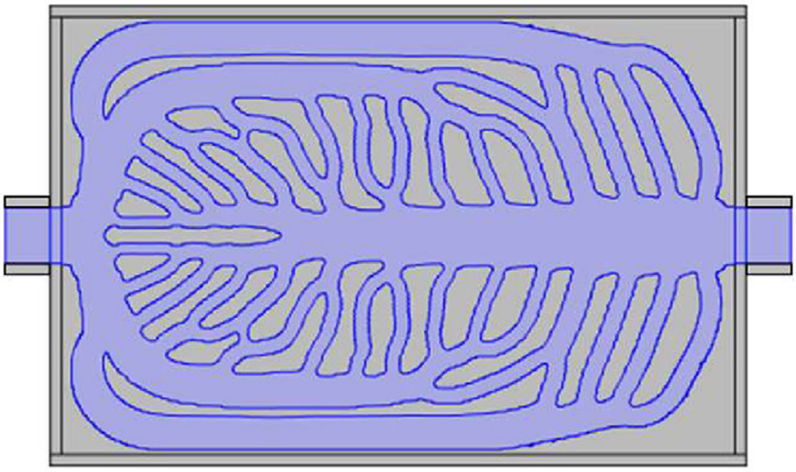

Figure 16: Topology optimized channels in cold plate with inlet and outlet in the centerline. Rectangular Cold Plate (RCP)

For a topology where the inlet and outlet are diagonal to each other, we get:

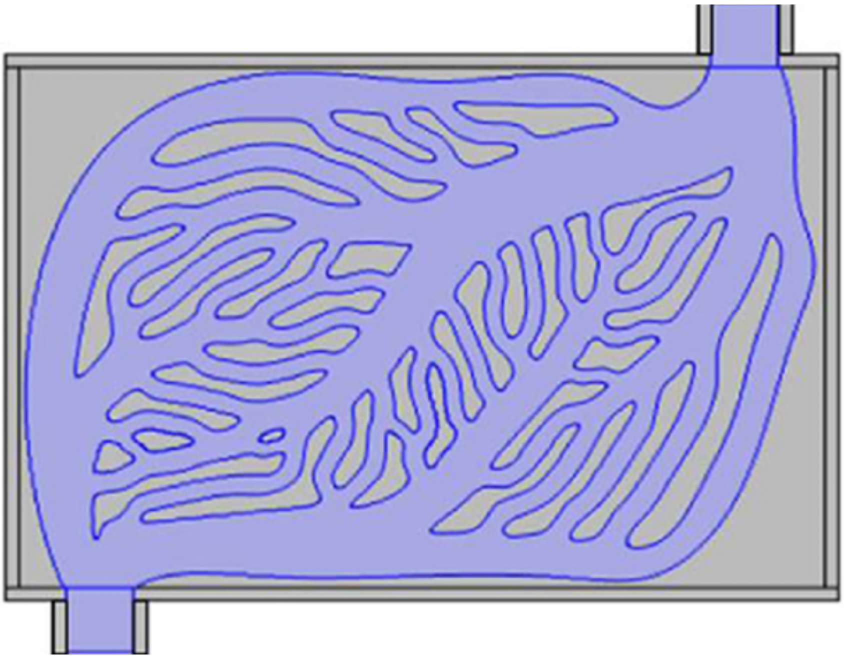

Figure 17: Diagonal in/outlets. Serpentine Cold Plate (SCP)

We do the usual, define boundary conditions, mesh, and compute, the results are discussed in the next section.

8 Theoretical vs Simulation results

8.1 Part 1: Fin design

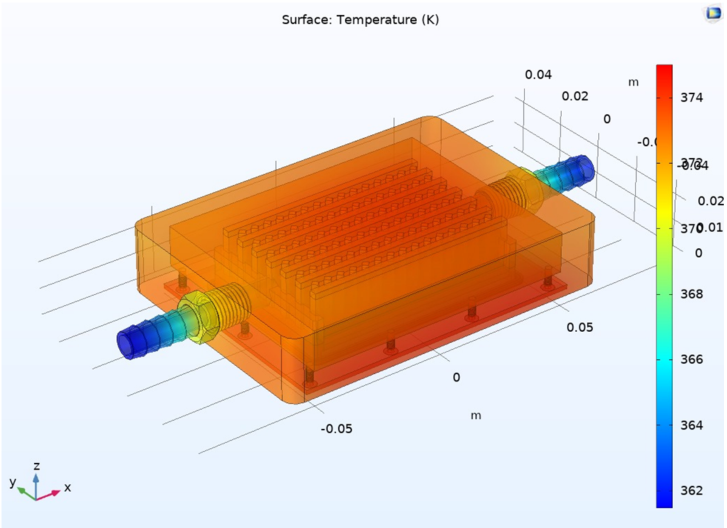

Figure 18: Temperature distribution over entire cold plate domain

The results for $T(x) vs x$ is as follows:

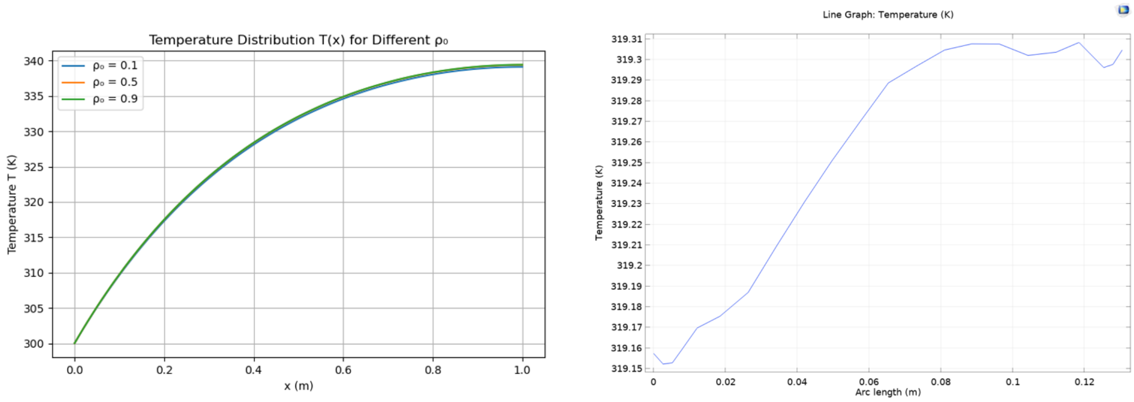

Figure 19

Which are in the same form as the theoretical results.

8.2 Part 2: Topology optimized design

Results before optimization vs after:

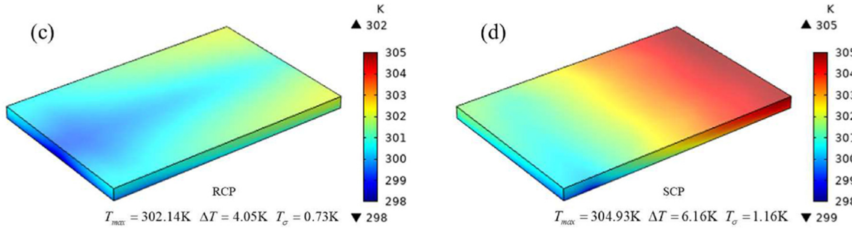

Figure 20: Before optimization

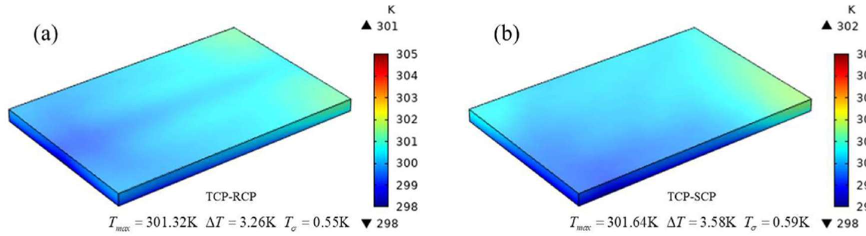

Figure 21: After optimization, especially great results with SCP.

And below are the theoretical results:

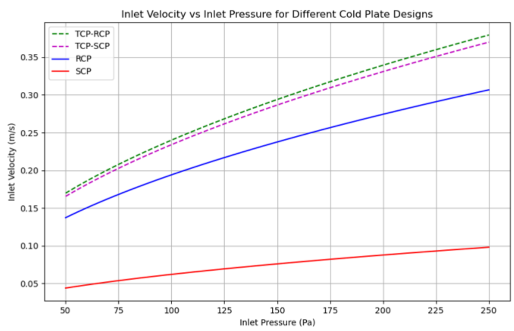

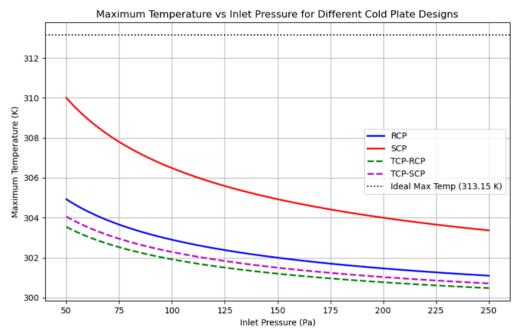

Compare them with simulation results:

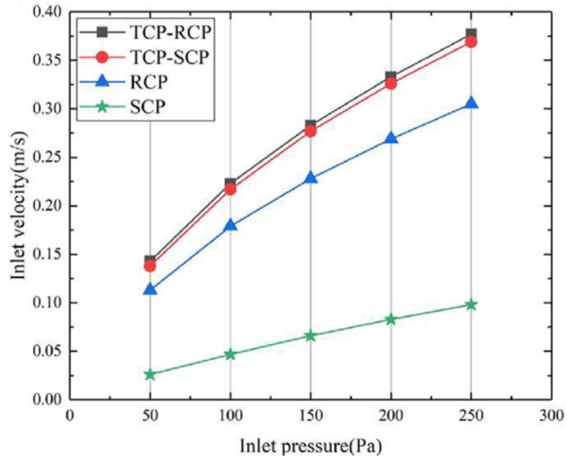

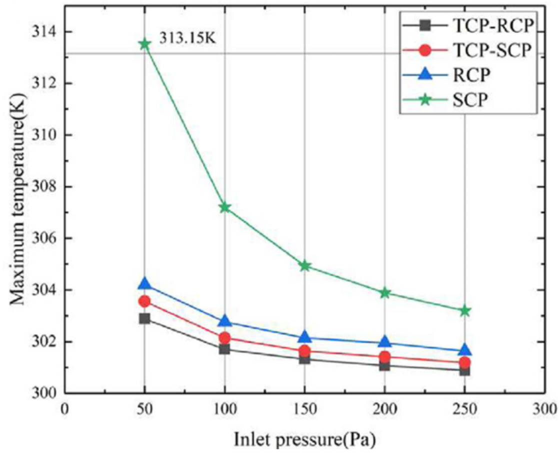

They yield the same curve.

9 Conclusion

This project has successfully designed, simulated, and optimized a cold plate for thermal management of electronics components. Ten different fin concepts were evaluated, and the Hybrid Pin-Fin and Channel design was selected as the optimal solution based on a comprehensive Figure ofiguret that balances thermal performance, pressure drop, and material efficiency.

References

1. ASME K-16/IEEE EPS Cold Plate Design Competition Guidelines, 2024-2025.

2. Incropera, F.P., DeWitt, D.P., Bergman, T.L., and Lavine, A.S., "Fundamentals of Heat and Mass Transfer," 7th Edition, John Wiley & Sons, 2011.

3. Kandlikar, S.G., and Grande, W.J., "Evolution of Microchannel Flow Passages - Thermohydraulic Performance and Fabrication Technology," Heat Transfer Engineering, Vol. 24, No. 1, pp. 3-17, 2003.

4. Lee, P.S., and Garimella, S.V., "Thermally Developing Flow and Heat Transfer in Rectangular Microchannels of Different Aspect Ratios," International Journal of Heat and Mass Transfer, Vol. 49, pp. 3060-3067, 2006.

5. Tuckerman, D.B., and Pease, R.F.W., "High-Performance Heat Sinking for VLSI," IEEE Electron Device Letters, Vol. EDL-2, No. 5, pp. 126-129, 1981.